Purpose

In this experiment, by carrying out the energy calibration, identification of elements appeared in PIXE spectra and determination of elemental concentration of thin samples, students will understand the principles of PIXE analysis.

Introduction

Particle-Induced X-ray Emission (PIXE) is the well-established nondestructive analytical techniques of X-ray emission spectroscopy. These techniques are powerful tools for rapid multielement nondestructive analyses and enable simultaneous detection of many elements in a solid or liquid with high-detection sensitivities, even in those cases where only small sample amounts are available. The elements are identified by the wavelengths (qualitative) of the emitted X-rays while the concentrations of the elements present in the sample are determined by the intensity of those X-rays (quantitative). PIXE has emerged as efficient and powerful analytical tools for major, minor, and trace elemental analysis in a variety of fields like biology, environment, medicine, archaeology, and forensic science. These techniques can be used for analyzing rocks, metals, ceramics, and other materials.

The principle of both of these techniques is to excite the atoms of the substance to be analyzed by bombarding the sample with sufficiently energetic charged particles. The ionization caused due to Coulomb-interaction in case of PIXE of inner- shell electrons is produced by charged particles. When this interaction removes an electron from a specimen's atom, frequently an electron from an outer shell (or orbital) occupies the vacancy. The distribution of electrons in the ionized atom is then out of equilibrium and within an extremely short time (~10^{-15} s) returns to the normal state, by transitions of electrons from outer to inner shells. When an outer-shell electron occupies a vacancy, it must lose a specific amount of energy to occupy the closer shell of more binding energy. This amount is readily predicted by the laws of Quantum Mechanics and usually much of the energy is emitted in the form of X-rays. Each of such electron transfer, for example from the L-shell to the K-shell, represents a loss in the potential energy of the atom. When released as an X-ray photon, the process is X-ray emission. This energy appears as a photon (in this case a Kα photon) whose energy is the difference between the binding energies of the filled outer shell and the vacant inner-shell. In the normal process of emission, an inner-shell electron is ejected producing the photoelectron. Similarly, in the ion-atom collisions one or more of the atomic electrons can get free (single or multiple ionization), one or several electrons can be transferred from one collision partner to the other, one or both of the collision partners can become excited, and a combination of these elementary processes can also take place. The excess energy is taken away by either photons (characteristic X-rays) - when an electron from a higher level falls into the inner-shell vacancy or Auger (higher-shell) electrons - when the energy released during the process of hole being filled by the outer shell electron, is transferred to another higher-shell electron. These emissions have characteristic energies determined fundamentally by the binding energy of the levels. The fraction of radiative (X-ray) decays is called the fluorescence yield, and is high for deep inner-shells. The de-excitation process leading to the emission of characteristic X-rays and Auger electrons is shown in Fig. 1. The Auger effect is most common with low-Z elements.

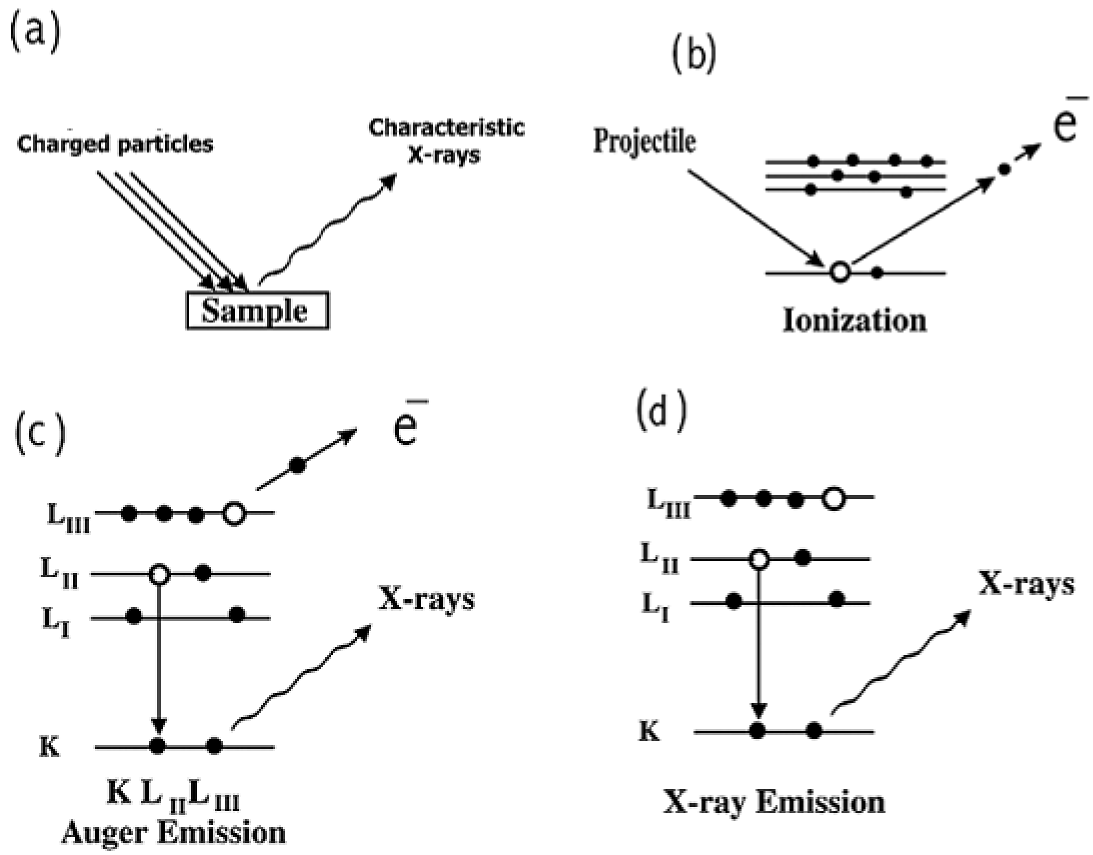

We have seen earlier that an electron from the K shell (or higher shell, if the energy of the impinging radiation (X-rays/y-rays) or charged particles is less than the binding energy of the K-shell) is ejected from the atom creating a vacancy in that shell as the projectile pass through the target atom. This vacancy is filled by an electron from the L or M shell. In the process, it emits a characteristic K X-ray unique to this element and in turn, produces a vacancy in the L or M shell.

The designation of various K and L X-ray transitions to denote transitions of electrons is given in Table 1 and Fig 2.

Table 1. Designation of various K and L X-ray transitions to denote transitions of electrons

K X-ray Lines	L X-ray Lines	
$K\alpha_1(K\text{-}L_{III})$	$Ll(L_{III}\text{-}M_1)$	$L\gamma_1(L_{II}\text{-}N_{IV})$
$K\alpha_2(K\text{-}L_{II})$	$L\alpha_{1,2}(L_{III}\text{-}M_{IV,V})$	$L\gamma_2(L_I\text{-}N_{II})$
$K\beta_1(K\text{-}M_{III})$	$L\beta_1(L_{II}\text{-}M_{IV})$	$L\gamma_3(L_I\text{-}N_{III})$
$K\beta_2(K\text{-}N_{II,III})$	$L\beta_2(L_{III}\text{-}N_V)$	$L\gamma_4(L_I\text{-}O_{III})$
$K\beta_3(K\text{-}M_{II})$	$L\beta_3(L_I\text{-}M_{III})$	$L\gamma_6(L_{II}\text{-}O_{IV})$

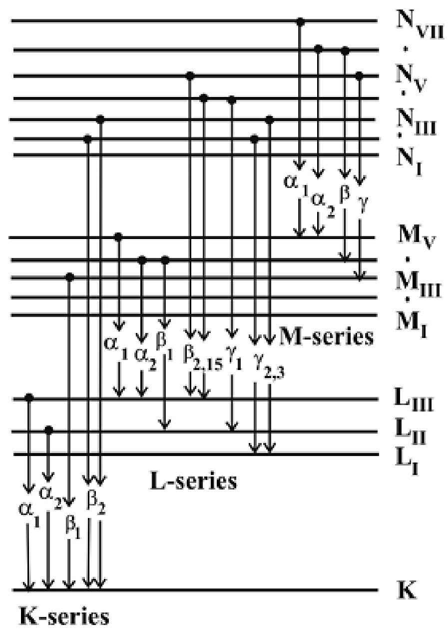

Fig. 2. Energy level diagram showing the origin of some of the K, L, and M X-rays

Energies of Characteristic X-ray can be found in the Appendix.

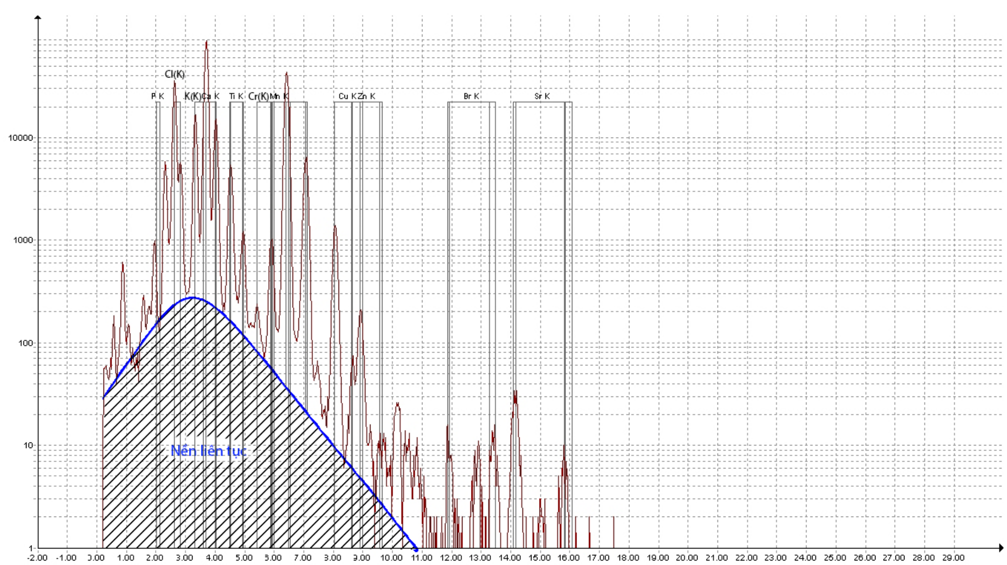

Fig.3. PIXE spectrum of a soil sample (Collected by HUS 5SDH-2 Tandem Pelletron Accelerator system)

PIXE spectrum consist of 2 components: Characteristic X-ray peaks overlying the continuous bremsstrahlung background (Just like towers builded over hillside)

Experiment 2
Particle-Induced X-Ray Emission (PIXE)

For PIXE analysis of thin target - a simplest case when the target is thin enough for corrections for projectile energy loss and X-ray absorption are negligibles. With this type of target, the concentration is replaced by the areal density (usually in $\mu g/cm^2$ or atom/cm^2). For each element with atomic number of Z presented in the sample, we have:

- The probability that a given ionization process for a specific inner- shell (K,L,M) will occur when an atom or molecule interacts with charged particles can be described in term of ionzation cross-section (in the unit of *barn*). It depends on the energy of projectiles E_0. Then the number of ionization events followed by the bombardment of N_p particles on the target with the areal density of N_t (in atom/cm^2) is:

$$Y_{ionnization} = N_p \sigma_Z(E_0) N_t$$

  This equation can be rewritten in term of $\mu g/cm^2$ unit:

$$Y_{ionization} = N_p \sigma_Z(E_0) \frac{N_{AV} M_A(Z)}{A_Z}$$

  - N_{AV} is Avogadro number
  - $M_A(Z)$ is the areal density in $\mu g/cm^2$
  - A_Z is the atomic number of element Z.

- The probability that aforementioned ionization event can caused the characteristic X-ray emission for a specific inner-shell (i.e. the probability that the vacant site created on an inner shell will be filled by an electron) is called fluorescence yield ω_Z. So the number of characteristic X-ray emission events is given by:

$$Y_{fluorescense} = Y_{ionization} \cdot \omega_Z$$

- Lets us call b_z the relative intensity which is equal to the number of characteristic X-ray of a particular X-ray line ($K\alpha_1$, $K\alpha_2$), divided by the number of characteristic X-ray emitted from a particular shell (K, L, M…). Then the number of X-ray emission for each line is given by:

$$Y_{characteristic} = Y_{fluorescense} \cdot b_Z$$

- The characteristic X-rays is recorded by X-ray detectors. There are several types of X-rays detectors can be used such as Si(Li), HpGe or Sillicon Drift Detector (SDD). Every detectors have their own intrinsic efficiency $\varepsilon_{intrinsic}$:

$$\varepsilon_{intrinsic} = \frac{number\ of\ radiation\ quanta\ recorded}{number\ of\ radiation\ quanta\ incident\ on\ detector}$$

  For a particular geometry, there is a specific solid angle Ω (in steradian unit) from the X-ray emission spot to sensitive area of the detector. Besides, between target and detector, there is a thin filter used to absorb a portion of intense low energy X-ray and suppress backscatted particles (which may cause high dead time and degradation of detector). Let's call T the transmission of the filter. We have:

$$Y_{characteristic\ X-ray\ recorded} = Y_{characteristic} \cdot \varepsilon_{intrinsic} \cdot \mathrm{T} \cdot \frac{\Omega}{4\pi}$$

  A reasonable transmission for Mylar can be obtained from the following:

$$T = e^{\frac{-470.168x}{E^{2.9897}}}$$

  Where E the energy of corresponding X-ray lines (in keV); x the thickness of the filter (in mm)

- Taken in to an account all above formulas, one can obtain the formula for determination of concentration of an element Z for thin target derived from the peak area of its characteristic X-ray as follow:

$$M_A(Z) = \frac{4\pi A_Z SH}{N_p \sigma_Z(E_0) N_{AV} \omega_Z b_Z \varepsilon_{intrinsic} T\Omega} \qquad (*)$$

In this formula, H value is a correction factor taken into an account all sources of systematic error.

The number of incident charged particles (with charge state +q) can be obtained by a charge collection system (usually consists of a Faraday cup and a current integrator) which records the total collected charge in the sample and following:

$$N_p = \frac{Q}{eq} \qquad (**)$$

Where e=1.60217646 × 10^{-19} C the elementary charge value.

Equipment required

- Tandem Pelletron Accelerator model 5SDH-2 with the maxmium terminal voltage of 1.7 MV
- X-ray spectroscopy: Sillicon Drift Detector (SDD), with the energy resolution of 138 eV at 5.9 keV X-ray emission from Mn, a compact electronics consisting of high voltage, pre-amplifier and amplifier, a multi channel analyzer (MCA) and a data aquasition computer.
- X-ray detector is placed at the angle of 32.8 degree with the beam direction.
- 2 samples (targets) are used:
  - A thin sample consists of CsBr with the areal density of 47.7 $\mu g/cm^2$ evaporated onto a thin Mylar foil (3.5 μm)
  - A thick standard sample named NIST 611 contained many trace elements in glass subtrate.

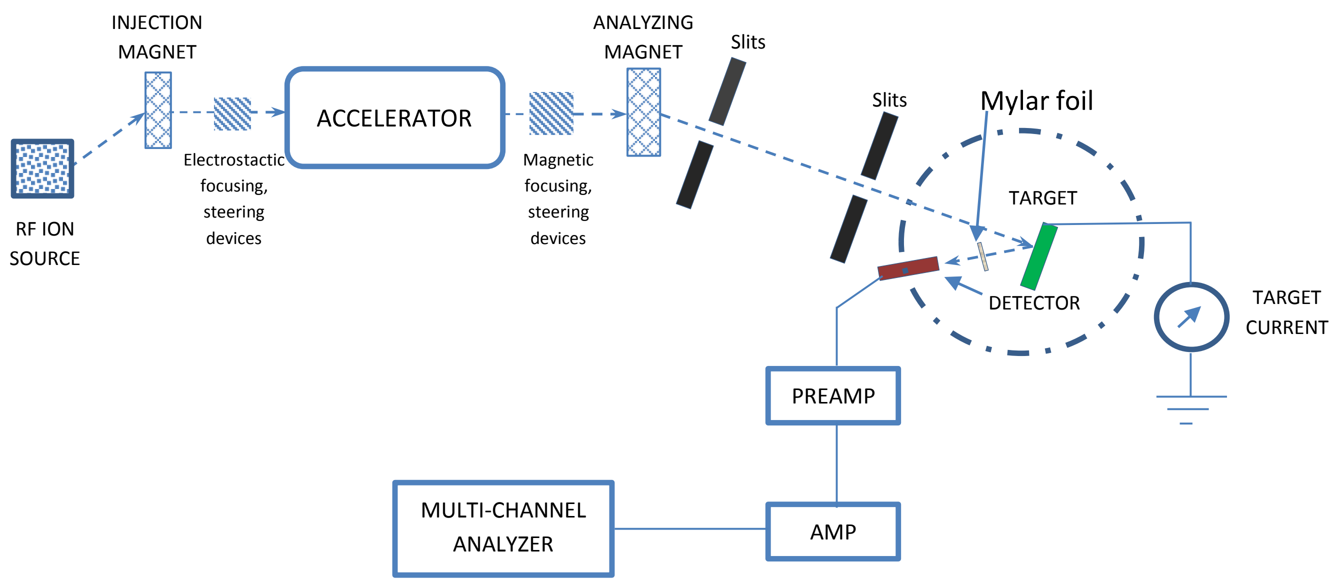

Hình 4. Experimental arrangement for PIXE experiment

Experiment 2
Particle-Induced X-Ray Emission (PIXE)

Procedures

1. Set up the experiment as shown in Fig 4, check all the connections.
2. Start the accelerator system, set up the accelerated beam with the following paramenters:
   - Beam type: H^+
   - Beam energy: 2.5 MeV
   - Beam intensity: <5 nA for CsBr sample, ~10-15 nA for NIST sample.
3. Adjust the position of the SDD detector (follow instructions) and recored the current geometry parameters.
4. Record the thickness of the filter.
5. Turn on the electronics of detection system.
6. Place the CsBr and NIST611 into the analysis chamber under vaccum (follow instructions)
7. Open the RC43 data aquasition program
   a. From the main window, click on the RC43 icons, 2 windows will appear.
   b. From NEC RC43 ANALYTICAL DATA COLLECTION window, choose DATA COLLECTION > Collect data.
   c. After A window named "Full Energy Data Collection" appears, unselect MCAs displayed options for RBG, RBS và NRA.
8. Adjust the beam intensity to a desired value for each sample.
9. Adjust the position of sample by using Manipulator window (in RC43 program) so that the interaction (illuminant) spot of the beam completely lies on the sample and the angle between surface normal and beam direction is equa to zero.
10. Preset the value of total charge collected (corresponding to the number of incident particles) in Full Energy Data Collection Window and name the spectrum in "Filename" textbox.
11. Recheck all the parameters and click on "Manual collect" button to start irradiation and spectrum aquasition. Observe the arising PIXE spectrum, show the contiuous background and charateristic X-rays.
12. When the measurement finishes, RC43 program will automatically store data in a file named before.
13. Obtain all the experimental parameters and the PIXE spectrum

Exercises

1. From PIXE spectrum of CsBr sample, perform an energy calibration of the detection system using charateristic X-ray lines $L\beta_1, L\beta_2, L\gamma_1$ of Cs and $K\beta_1$ of Br.
2. Using calculated values of energy calibration and PIXE spectrum of the NIST611 sample, identify elements which may present in the sample.
3. Use the (*) and (**) fomulas, experimental parameters and PIXE spectrum of thin CsBr sample to determine the concentration (in the unit of areal density) of Br. Compare the calculated value of Br concentration with nominal value. Make a comment.

Questions

1. Give the mechanism of bremsstrahlung emission?
2. Give the mechanism of X-ray attenuation and slowing down of charged particles in materials (related to the use of the Mylar filter)
3. What would happen if thick sample (i.e. Incident paticles stop completely in the sample) is used?

X-Ray Data Booklet Table 1-2. *Photon energies, in electron volts, of principal K-, L-, and M-shell emission lines.*

Element	$K\alpha_1$	$K\alpha_2$	$K\beta_1$	$L\alpha_1$	$L\alpha_2$	$L\beta_1$	$L\beta_2$	$L\gamma_1$	$M\alpha_1$
3 Li	54.3								
4 Be	108.5								
5 B	183.3								
6 C	277								
7 N	392.4								
8 O	524.9								
9 F	676.8								
10 Ne	848.6	848.6							
11 Na	1,040.98	1,040.98	1,071.1						
12 Mg	1,253.60	1,253.60	1,302.2						
13 Al	1,486.70	1,486.27	1,557.45						
14 Si	1,739.98	1,739.38	1,835.94						
15 P	2,013.7	2,012.7	2,139.1						
16 S	2,307.84	2,306.64	2,464.04						
17 Cl	2,622.39	2,620.78	2,815.6						
18 Ar	2,957.70	2,955.63	3,190.5						
19 K	3,313.8	3,311.1	3,589.6						
20 Ca	3,691.68	3,688.09	4,012.7	341.3	341.3	344.9			
21 Sc	4,090.6	4,086.1	4,460.5	395.4	395.4	399.6			

Table 1-2. ***Energies of x-ray emission lines (continued).***

Element	$K\alpha_1$	$K\alpha_2$	$K\beta_1$	$L\alpha_1$	$L\alpha_2$	$L\beta_1$	$L\beta_2$	$L\gamma_1$	$M\alpha_1$
22 Ti	4,510.84	4,504.86	4,931.81	452.2	452.2	458.4			
23 V	4,952.20	4,944.64	5,427.29	511.3	511.3	519.2			
24 Cr	5,414.72	5,405.509	5,946.71	572.8	572.8	582.8			
25 Mn	5,898.75	5,887.65	6,490.45	637.4	637.4	648.8			
26 Fe	6,403.84	6,390.84	7,057.98	705.0	705.0	718.5			
27 Co	6,930.32	6,915.30	7,649.43	776.2	776.2	791.4			
28 Ni	7,478.15	7,460.89	8,264.66	851.5	851.5	868.8			
29 Cu	8,047.78	8,027.83	8,905.29	929.7	929.7	949.8			
30 Zn	8,638.86	8,615.78	9,572.0	1,011.7	1,011.7	1,034.7			
31 Ga	9,251.74	9,224.82	10,264.2	1,097.92	1,097.92	1,124.8			
32 Ge	9,886.42	9,855.32	10,982.1	1,188.00	1,188.00	1,218.5			
33 As	10,543.72	10,507.99	11,726.2	1,282.0	1,282.0	1,317.0			
34 Se	11,222.4	11,181.4	12,495.9	1,379.10	1,379.10	1,419.23			
35 Br	11,924.2	11,877.6	13,291.4	1,480.43	1,480.43	1,525.90			
36 Kr	12,649	12,598	14,112	1,586.0	1,586.0	1,636.6			
37 Rb	13,395.3	13,335.8	14,961.3	1,694.13	1,692.56	1,752.17			
38 Sr	14,165	14,097.9	15,835.7	1,806.56	1,804.74	1,871.72			
39 Y	14,958.4	14,882.9	16,737.8	1,922.56	1,920.47	1,995.84			
40 Zr	15,775.1	15,690.9	17,667.8	2,042.36	2,039.9	2,124.4	2,219.4	2,302.7	

41 Nb	16,615.1	16,521.0	18,622.5	2,165.89	2,163.0	2,257.4	2,367.0	2,461.8	
42 Mo	17,479.34	17,374.3	19,608.3	2,293.16	2,289.85	2,394.81	2,518.3	2,623.5	
43 Tc	18,367.1	18,250.8	20,619	2,424	2,420	2,538	2,674	2,792	
44 Ru	19,279.2	19,150.4	21,656.8	2,558.55	2,554.31	2,683.23	2,836.0	2,964.5	
45 Rh	20,216.1	20,073.7	22,723.6	2,696.74	2,692.05	2,834.41	3,001.3	3,143.8	
46 Pd	21,177.1	21,020.1	23,818.7	2,838.61	2,833.29	2,990.22	3,171.79	3,328.7	
47 Ag	22,162.92	21,990.3	24,942.4	2,984.31	2,978.21	3,150.94	3,347.81	3,519.59	
48 Cd	23,173.6	22,984.1	26,095.5	3,133.73	3,126.91	3,316.57	3,528.12	3,716.86	
49 In	24,209.7	24,002.0	27,275.9	3,286.94	3,279.29	3,487.21	3,713.81	3,920.81	
50 Sn	25,271.3	25,044.0	28,486.0	3,443.98	3,435.42	3,662.80	3,904.86	4,131.12	
51 Sb	26,359.1	26,110.8	29,725.6	3,604.72	3,595.32	3,843.57	4,100.78	4,347.79	
52 Te	27,472.3	27,201.7	30,995.7	3,769.33	3,758.8	4,029.58	4,301.7	4,570.9	
53 I	28,612.0	28,317.2	32,294.7	3,937.65	3,926.04	4,220.72	4,507.5	4,800.9	
54 Xe	29,779	29,458	33,624	4,109.9	—	—	—	—	
55 Cs	30,972.8	30,625.1	34,986.9	4,286.5	4,272.2	4,619.8	4,935.9	5,280.4	
56 Ba	32,193.6	31,817.1	36,378.2	4,466.26	4,450.90	4,827.53	5,156.5	5,531.1	
57 La	33,441.8	33,034.1	37,801.0	4,650.97	4,634.23	5,042.1	5,383.5	5,788.5	833
58 Ce	34,719.7	34,278.9	39,257.3	4,840.2	4,823.0	5,262.2	5,613.4	6,052	883
59 Pr	36,026.3	35,550.2	40,748.2	5,033.7	5,013.5	5,488.9	5,850	6,322.1	929
60 Nd	37,361.0	36,847.4	42,271.3	5,230.4	5,207.7	5,721.6	6,089.4	6,602.1	978
61 Pm	38,724.7	38,171.2	43,826	5,432.5	5,407.8	5,961	6,339	6,892	—
62 Sm	40,118.1	39,522.4	45,413	5,636.1	5,609.0	6,205.1	6,586	7,178	1,081

Table 1-2. *Energies of x-ray emission lines (continued).*

Element	$K\alpha_1$	$K\alpha_2$	$K\beta_1$	$L\alpha_1$	$L\alpha_2$	$L\beta_1$	$L\beta_2$	$L\gamma_1$	$M\alpha_1$
63 Eu	41,542.2	40,901.9	47,037.9	5,845.7	5,816.6	6,456.4	6,843.2	7,480.3	1,131
64 Gd	42,996.2	42,308.9	48,697	6,057.2	6,025.0	6,713.2	7,102.8	7,785.8	1,185
65 Tb	44,481.6	43,744.1	50,382	6,272.8	6,238.0	6,978	7,366.7	8,102	1,240
66 Dy	45,998.4	45,207.8	52,119	6,495.2	6,457.7	7,247.7	7,635.7	8,418.8	1,293
67 Ho	47,546.7	46,699.7	53,877	6,719.8	6,679.5	7,525.3	7,911	8,747	1,348
68 Er	49,127.7	48,221.1	55,681	6,948.7	6,905.0	7,810.9	8,189.0	9,089	1,406
69 Tm	50,741.6	49,772.6	57,517	7,179.9	7,133.1	8,101	8,468	9,426	1,462
70 Yb	52,388.9	51,354.0	59,370	7,415.6	7,367.3	8,401.8	8,758.8	9,780.1	1,521.4
71 Lu	54,069.8	52,965.0	61,283	7,655.5	7,604.9	8,709.0	9,048.9	10,143.4	1,581.3
72 Hf	55,790.2	54,611.4	63,234	7,899.0	7,844.6	9,022.7	9,347.3	10,515.8	1,644.6
73 Ta	57,532	56,277	65,223	8,146.1	8,087.9	9,343.1	9,651.8	10,895.2	1,710
74 W	59,318.24	57,981.7	67,244.3	8,397.6	8,335.2	9,672.35	9,961.5	11,285.9	1,775.4
75 Re	61,140.3	59,717.9	69,310	8,652.5	8,586.2	10,010.0	10,275.2	11,685.4	1,842.5
76 Os	63,000.5	61,486.7	71,413	8,911.7	8,841.0	10,355.3	10,598.5	12,095.3	1,910.2
77 Ir	64,895.6	63,286.7	73,560.8	9,175.1	9,099.5	10,708.3	10,920.3	12,512.6	1,979.9
78 Pt	66,832	65,112	75,748	9,442.3	9,361.8	11,070.7	11,250.5	12,942.0	2,050.5
79 Au	68,803.7	66,989.5	77,984	9,713.3	9,628.0	11,442.3	11,584.7	13,381.7	2,122.9
80 Hg	70,819	68,895	80,253	9,988.8	9,897.6	11,822.6	11,924.1	13,830.1	2,195.3
81 Tl	72,871.5	70,831.9	82,576	10,268.5	10,172.8	12,213.3	12,271.5	14,291.5	2,270.6

82	Pb	74,969.4	72,804.2	84,936	10,551.5	10,449.5	12,613.7	12,622.6	14,764.4	2,345.5
83	Bi	77,107.9	74,814.8	87,343	10,838.8	10,730.91	13,023.5	12,979.9	15,247.7	2,422.6
84	Po	79,290	76,862	89,800	11,130.8	11,015.8	13,447	13,340.4	15,744	—
85	At	81,520	78,950	92,300	11,426.8	11,304.8	13,876	—	16,251	—
86	Rn	83,780	81,070	94,870	11,727.0	11,597.9	14,316	—	16,770	—
87	Fr	86,100	83,230	97,470	12,031.3	11,895.0	14,770	14,450	17,303	—
88	Ra	88,470	85,430	100,130	12,339.7	12,196.2	15,235.8	14,841.4	17,849	—
89	Ac	90,884	87,670	102,850	12,652.0	12,500.8	15,713	—	18,408	—
90	Th	93,350	89,953	105,609	12,968.7	12,809.6	16,202.2	15,623.7	18,982.5	2,996.1
91	Pa	95,868	92,287	108,427	13,290.7	13,122.2	16,702	16,024	19,568	3,082.3
92	U	98,439	94,665	111,300	13,614.7	13,438.8	17,220.0	16,428.3	20,167.1	3,170.8
93	Np	—	—	—	13,944.1	13,759.7	17,750.2	16,840.0	20,784.8	—
94	Pu	—	—	—	14,278.6	14,084.2	18,293.7	17,255.3	21,417.3	—
95	Am	—	—	—	14,617.2	14,411.9	18,852.0	17,676.5	22,065.2	—

TABLE 2. *K*-shell x-ray production by protons in target elements from beryllium to uranium[a,b]—Continued

E_1 (MeV)	σ^{Exper} (barn)	$\sigma^{Exper}/\sigma^{ECPSSR}$	E_1 (MeV)	σ^{Exper} (barn)	$\sigma^{Exper}/\sigma^{ECPSSR}$	E_1 (MeV)	σ^{Exper} (barn)	$\sigma^{Exper}/\sigma^{ECPSSR}$	Ref.
1.00+0	2.00+0	1.11+0	2.00+0	1.50+1	1.11+0				39
4.00-1	7.16-2	1.22+0	6.00-1	2.91-1	9.70-1	8.00-1	8.49-1	9.97-1	61
1.00+0	1.86+0	1.03+0	1.20+0	2.81+0	8.77-1	1.40+0	4.41+0	8.68-1	
1.60+0	6.54+0	8.80-1	1.80+0	8.57+0	8.37-1	2.00+0	1.15+1	8.54-1	
3.00+0	3.42+1	9.92-1							94
1.00+1	2.26+2	1.17+0	1.20+1	2.74+2	1.24+0	1.40+1	2.80+2	1.16+0	
1.60+1	2.98+2	1.17+0	1.80+1	3.22+2	1.22+0	2.00+1	3.28+2	1.21+0	
2.20+1	3.10+2	1.12+0							
6.00-1	3.19-1	1.06+0	8.00-1	8.28-1	9.72-1	1.00+0	1.79+0	9.93-1	113
1.20+0	3.18+0	9.92-1	1.40+0	4.89+0	9.62-1	1.60+0	7.21+0	9.70-1	
1.80+0	1.04+1	1.02+0	2.00+0	1.34+1	9.95-1	2.20+0	1.62+1	9.52-1	
2.40+0	1.90+1	9.04-1							
7.00+0	1.50+2	1.10+0							114
2.00-1	2.08-3	1.19+0	2.50-1	6.20-3	9.97-1	3.00-1	1.44-2	9.16-1	115
3.50-1	3.59-2	1.11+0	4.00-1	5.86-2	1.00+0	4.50-1	9.12-2	9.48-1	
5.00-1	1.52-1	1.03+0	6.00-1	3.06-1	1.02+0	7.00-1	5.46-1	1.03+0	
8.00-1	8.70-1	1.02+0	9.00-1	1.28+0	1.01+0	1.00+0	1.79+0	9.93-1	
1.10+0	2.39+0	9.78-1	1.20+0	3.15+0	9.83-1	1.30+0	4.02+0	9.84-1	
1.40+0	5.05+0	9.94-1	1.50+0	5.88+0	9.48-1	1.60+0	7.39+0	9.94-1	
1.70+0	8.46+0	9.63-1	1.80+0	9.83+0	9.60-1	1.90+0	1.13+1	9.57-1	
2.00+0	1.28+1	9.51-1							
7.00+0	1.54+2	1.13+0							125
35 Bromine			Fluorescence yield = 0.615						
6.00-1	3.34-1	1.50+0	8.00-1	7.93-1	1.24+0	1.00+0	1.56+0	1.14+0	61
1.20+0	2.71+0	1.10+0	1.40+0	4.47+0	1.13+0	1.60+0	6.03+0	1.04+0	
1.80+0	8.31+0	1.03+0	2.00+0	1.04+1	9.75-1				
1.50+0	4.00+0	8.29-1	2.00+0	9.95+0	9.33-1	2.25+0	1.29+1	9.00-1	143
2.50+0	1.74+1	9.37-1	2.75+0	2.18+1	9.45-1	3.00+0	2.95+1	1.05+0	
36 Krypton			Fluorescence yield = 0.643						
1.50+0	5.90+0	1.56+0	2.00+0	1.30+1	1.54+0	2.50+0	2.10+1	1.41+0	40
3.00+0	4.30+1	1.89+0	3.50+0	4.70+1	1.48+0	4.00+0	6.20+1	1.50+0	
4.50+0	7.70+1	1.50+0							
1.50+0	6.23+0	1.65+0	2.00+0	1.32+1	1.56+0	2.50+0	2.25+1	1.51+0	48
3.00+0	3.66+1	1.61+0	3.50+0	4.74+1	1.49+0	4.00+0	6.38+1	1.55+0	
4.50+0	7.92+1	1.55+0	5.00+0	1.02+2	1.67+0				
3.00+0	3.15+1	1.38+0							65
5.00-1	7.10-2	8.88-1	8.16-1	5.20-1	9.97-1	9.15-1	7.00-1	8.99-1	68
1.00+0	1.00+0	9.50-1	1.29+0	2.20+0	9.20-1	1.63+0	4.30+0	8.95-1	
2.00+0	6.80+0	8.03-1							

Table A16.8. K- and L-subshell fluorescence yields and Coster–Kronig probabilities. The K fluorescence yields are from a semiempirical fit by W. Bambyneks to selected experimental data reported in Hubbell, J. H., Trehan, P. N., Singh, N., Chand, B., Mehta, D., Garg, M. L., Garg, R. R., Singh, S., and Puri, S. (1994), *J. Phys. Chem. Ref. Data* **23**, 339. The **bold** L-shell quantities are from Krause, M. O. (1979), *J. Phys. Chem. Ref. Data* **8**, 307. The remainder of the L-shell quantities are from Campbell, J. L. (2003), *At. Data Nucl. Data Tables* **85**, 291 and Campbell, J. L. (2009) *At. Data Nucl. Data Tables* **95**, 115.

Z	ω_K	ω_{L1}	ω_{L2}	ω_{L3}	f_{12}	f_{13}	f_{23}
3	0.000293						
4	0.000693						
5	0.00141						
6	0.00258						
7	0.00435						
8	0.00691						
9	0.0104						
10	0.0152						
11	0.0213						
12	0.0291						
13	0.0387						
14	0.0504						
15	0.0642						
16	0.0804						
17	0.0989						
18	0.1199						
19	0.1432						
20	0.1687						
21	0.1962						
22	0.2256						
23	0.2564						
24	0.2885						
25	0.3213	**0.00084**	**0.005**	**0.005**	**0.3**	**0.58**	
26	0.3546	**0.001**	**0.0063**	**0.0063**	**0.3**	**0.57**	
27	0.3880	**0.0012**	**0.0077**	**0.0077**	**0.3**	**0.56**	
28	0.4212	**0.0014**	**0.0086**	**0.0093**	**0.3**	**0.55**	**0.028**
29	0.4538	**0.0016**	**0.01**	**0.011**	**0.3**	**0.54**	**0.028**
30	0.4857	**0.0018**	**0.011**	**0.012**	**0.29**	**0.54**	**0.026**
31	0.5166	**0.021**	**0.012**	**0.013**	**0.29**	**0.53**	**0.032**
32	0.5464	**0.0024**	**0.013**	**0.015**	**0.28**	**0.53**	**0.05**
33	0.5748	**0.0028**	**0.014**	**0.016**	**0.28**	**0.53**	**0.063**
34	0.6019	**0.0032**	**0.016**	**0.018**	**0.28**	**0.52**	**0.076**
35	0.6275	**0.0036**	**0.018**	**0.02**	**0.28**	**0.52**	**0.088**
36	0.6517	**0.0041**	**0.02**	**0.022**	**0.27**	**0.52**	**0.073**
37	0.6744	**0.0046**	**0.022**	**0.024**	**0.27**	**0.52**	0.08
38	0.6956	**0.0051**	**0.024**	**0.026**	**0.27**	**0.52**	0.087
39	0.7155	**0.0059**	**0.026**	**0.028**	**0.26**	**0.52**	0.094
40	0.7340	**0.0068**	**0.028**	**0.031**	**0.26**	**0.52**	0.1

Table A16.8. K- and L-subshell fluorescence yields and Coster–Kronig probabilities. The K fluorescence yields are from a semiempirical fit by W. Bambyneks to selected experimental data reported in Hubbell, J. H., Trehan, P. N., Singh, N., Chand, B., Mehta, D., Garg, M. L., Garg, R. R., Singh, S., and Puri, S. (1994), *J. Phys. Chem. Ref. Data* **23**, 339. The **bold** L-shell quantities are from Krause, M. O. (1979), *J. Phys. Chem. Ref. Data* **8**, 307. The remainder of the L-shell quantities are from Campbell, J. L. (2003), *At. Data Nucl. Data Tables* **85**, 291 and Campbell, J. L. (2009) *At. Data Nucl. Data Tables* **95**, 115 (continued).

Z	ω_K	ω_{L1}	ω_{L2}	ω_{L3}	f_{12}	f_{13}	f_{23}
41	0.7512	**0.0094**	**0.031**	**0.034**	**0.1**	**0.61**	0.106
42	0.7672	**0.01**	**0.034**	**0.037**	**0.1**	**0.61**	0.112
43	0.7821	**0.011**	**0.037**	**0.04**	**0.1**	**0.61**	0.118
44	0.7958	**0.012**	**0.04**	**0.043**	**0.1**	**0.61**	0.124
45	0.8086	**0.013**	**0.043**	**0.046**	**0.1**	**0.6**	0.13
46	0.8204	**0.014**	**0.047**	**0.049**	**0.1**	**0.6**	0.138
47	0.8313	**0.016**	**0.051**	**0.052**	**0.1**	**0.59**	0.141
48	0.8415	**0.018**	**0.056**	**0.056**	**0.1**	**0.59**	0.143
49	0.8508	**0.02**	**0.061**	**0.06**	**0.1**	**0.59**	0.146
50	0.8595	**0.037**	**0.065**	**0.064**	**0.17**	**0.59**	0.148
51	0.8676	**0.039**	**0.069**	**0.069**	**0.17**	**0.27**	0.151
52	0.8750	**0.041**	**0.074**	**0.074**	**0.18**	**0.28**	0.153
53	0.8819	**0.044**	**0.079**	**0.079**	**0.18**	**0.28**	0.156
54	0.8883	**0.046**	**0.083**	**0.085**	**0.19**	**0.28**	0.159
55	0.8942	**0.049**	**0.09**	**0.091**	**0.19**	**0.28**	0.159
56	0.8997	**0.052**	**0.096**	**0.097**	**0.19**	**0.28**	0.159
57	0.9049	**0.055**	**0.103**	**0.104**	**0.19**	**0.29**	0.159
58	0.9096	**0.058**	**0.11**	**0.111**	**0.19**	**0.29**	0.158
59	0.9140	**0.061**	**0.117**	**0.118**	**0.19**	**0.29**	0.158
60	0.9181	**0.064**	**0.136**	**0.134**	**0.19**	**0.3**	0.158
61	0.9220	**0.066**	0.145	0.142	**0.19**	**0.3**	0.156
62	0.9255	**0.071**	0.155	0.15	**0.19**	**0.3**	0.154
63	0.9289	**0.075**	0.164	0.158	**0.19**	**0.3**	0.152
64	0.9320	**0.102**	0.175	0.167	**0.19**	**0.279**	0.150
65	0.9349	0.107	0.186	0.175	0.182	0.285	0.148
66	0.9376	0.111	0.197	0.184	0.174	0.29	0.146
67	0.9401	0.116	0.208	0.193	0.166	0.296	0.144
68	0.9425	0.121	0.219	0.203	0.158	0.301	0.143
69	0.9447	0.131	0.231	0.212	0.15	0.306	0.141
70	0.9467	0.134	0.243	0.222	0.142	0.312	0.140
71	0.9487	0.138	0.256	0.231	0.134	0.317	0.138
72	0.9505	0.141	0.268	0.241	0.126	0.322	0.136
73	0.9522	0.144	0.28	0.251	0.118	0.328	0.134
74	0.9538	0.148	0.291	0.261	0.11	0.333	0.132
75	0.9553		0.304	0.271		0.482	0.131
76	0.9567		0.318	0.282		0.482	0.130
77	0.9580	0.145	0.331	0.292	0.076	0.482	0.128
78	0.9592	0.114	0.344	0.303	0.075	0.545	0.126
79	0.9604	0.117	0.358	0.313	0.074	0.615	0.125
80	0.9615	0.121	0.37	0.322	0.072	0.615	0.123

Table A16.8. K- and L-subshell fluorescence yields and Coster–Kronig probabilities. The K fluorescence yields are from a semiempirical fit by W. Bambyneks to selected experimental data reported in Hubbell, J. H., Trehan, P. N., Singh, N., Chand, B., Mehta, D., Garg, M. L., Garg, R. R., Singh, S., and Puri, S. (1994), *J. Phys. Chem. Ref. Data* **23**, 339. The **bold** L-shell quantities are from Krause, M. O. (1979), *J. Phys. Chem. Ref. Data* **8**, 307. The remainder of the L-shell quantities are from Campbell, J. L. (2003), *At. Data Nucl. Data Tables* **85**, 291 and Campbell, J. L. (2009) *At. Data Nucl. Data Tables* **95**, 115 (continued).

Z	ω_K	ω_{L1}	ω_{L2}	ω_{L3}	f_{12}	f_{13}	f_{23}
81	0.9625	0.124	0.384	0.332	0.069	0.615	0.121
82	0.9634	0.128	0.397	0.343	0.066	0.62	0.119
83	0.9643	0.132	0.411	0.353	0.063	0.62	0.117
84	0.9652	0.135	0.424	0.363	0.06	0.62	0.115
85	0.9659	0.138	0.438	0.374	0.057	0.62	0.113
86	0.9667	0.142	0.451	0.384	0.053	0.62	0.111
87	0.9674	0.146	0.464	0.394	0.05	0.62	0.109
88	0.9680	0.15	0.476	0.404	0.047	0.62	0.107
89	0.9686	0.154	0.49	0.414	0.044	0.62	0.105
90	0.9691	0.159	0.503	0.424	0.04	0.62	0.103
91	0.9696	0.164	0.495	0.434	0.038	0.62	0.141
92	0.9701	0.168	0.506	0.444	0.035	0.62	0.140

Table A16.9. Cross sections (barns) for K-shell ionization by protons as a function of atomic number Z and energy (MeV). From Chen, M.-H., and Crasemann, B. (1985), *At. Data Nucl. Data Tables* **33**, 217, and Chen, M.-H., and Crasemann, B. (1989), *At. Data Nucl. Data Tables* **41**, 257.

E (MeV)	22	26	29	30	32
0.10	4.440E–02	2.953E–03	3.884E–04	1.928E–04	4.598E–05
0.20	1.960E+00	1.416E–01	3.234E–02	1.990E–02	7.614E–03
0.30	5.771E+00	8.120E–01	2.149E–01	1.392E–01	6.018E–02
0.40	1.577+01	2.440E+00	6.944E–01	4.631E–01	2.107E–01
0.50	3.258E+01	5.392E+00	1.604E+00	1.088E+00	5.114E–01
0.60	5.671E+01	9.905E+00	3.063E+00	2.095E+00	1.012E+00
0.70	8.852E+01	1.614E+01	5.141E+00	3.561E+00	1.746E+00
0.80	1.273E+02	2.426E+01	7.900E+00	5.517E+00	2.747E+00
0.90	1.731E+02	3.416E+01	1.141E+01	7.999E+00	4.037E+00
1.00	2.245E+02	4.597E+01	1.563E+01	1.106E+01	5.648E+00
1.25	3.742E+02	8.254E+01	2.945E+01	2.106E+01	1.104E+01
1.50	5.445E+02	1.283E+02	4.746E+01	3.445E+01	1.845E+01
1.75	7.252E+02	1.811E+02	6.935E+01	5.072E+01	2.769E+01
2.00	9.068E+02	2.383E+02	9.434E+01	6.967E+01	3.870E+01
2.25	1.088E+03	2.993E+02	1.215E+02	9.048E+01	5.106E+01
2.50	1.260E+03	3.612E+02	1.504E+02	1.132E+02	6.478E+01
2.75	1.427E+03	4.244E+02	1.809E+02	1.367E+02	7.932E+01
3.00	1.580E+03	4.862E+02	2.117E+02	1.615E+02	
3.25	1.731E+03	5.484E+02	2.434E+02	1.864E+02	1.107E+02
3.50	1.864E+03	6.076E+02	2.746E+02	2.114E+02	1.270E+02
3.75	1.992E+03	6.645E+02	3.054E+02	2.370E+02	1.438E+02
4.00	2.105E+03	7.208E+02	3.366E+02	2.619E+02	1.604E+02
4.25	2.208E+03	7.732E+02	3.664E+02	2.864E+02	1.769E+02
4.50	2.307E+03	8.230E+02	3.954E+02	3.112E+02	1.934E+02
4.75	2.393E+03	8.723E+02	4.246E+02	3.347E+02	2.102E+02
5.00	2.471E+03	9.171E+02	4.519E+02	3.576E+02	2.262E+02

Table A16.1. K X-ray energies and relative intensities for elements 6 ≤ Z ≤ 60. If a label does not appear in the leftmost column, then that transition does not occur for any of the elements in that block; if no energy is listed for a transition, then that transition does not occur for that specific element. The column headers contain the atomic symbol and the atomic mass (g/mol) of the elements. The two columns of data for each element contain the energy of the transition line in keV and the relative intensity of each line, respectively. The intensities sum to 1.0. Doublets having very small energy separations are combined. The radiative Auger satellites are also included where pertinent (continued).

Line	**Ga 69.72**		**Ge 72.59**		**As 74.92**		**Se 78.96**		**Br 79.91**	
KL_2 ($K\alpha_2$)	9.225	0.2971	9.855	0.2957	10.508	0.2946	11.182	0.2933	11.878	0.2926
KL_3 ($K\alpha_1$)	9.252	0.5775	9.886	0.5743	10.544	0.5717	11.222	0.5683	11.924	0.5647
K_{LM}	9.094	0.0012	9.706	0.0012	10.340	0.0011	10.990	0.0011	11.667	0.0011
KM_2 ($K\beta_3$)	10.260	0.0414	10.975	0.0421	11.720	0.0429	12.490	0.0437	13.284	0.0443
KM_3 ($K\beta_1$)	10.264	0.0810	10.982	0.0825	11.726	0.0839	12.496	0.0855	13.292	0.0865
KM_4 ($K\beta_5^{II}$)	10.346	0.0002	11.074	0.0001		0.0		0.0		0.0
KM_5 ($K\beta_5^{I}$)	10.351	0.0003	11.075	0.0002		0.0		0.0		0.0
K_{MM}	10.072	0.0013	10.769	0.0012	11.523	0.0011	12.264	0.0010	13.036	0.0010
KN_2 ($K\beta_2^{II}$)		0.0	11.101	0.0009	11.864	0.0016	12.652	0.0024	13.469	0.0034
KN_3 ($K\beta_2^{I}$)		0.0	11.103	0.0018	11.864	0.0031	12.652	0.0047	13.469	0.0065

Line	**Kr 83.80**		**Rb 85.47**		**Sr 87.62**		**Y 88.90**		**Zr 91.22**	
KL_2 ($K\alpha_2$)	12.598	0.2916	13.336	0.2907	14.098	0.2899	14.883	0.2893	15.691	0.2884
KL_3 ($K\alpha_1$)	12.651	0.5628	13.395	0.5598	14.165	0.5569	14.958	0.5544	15.775	0.5520
K_{LM}	12.359	0.0010	13.073	0.0010	13.807	0.0009	14.565	0.0009	15.345	0.0009
KM_2 ($K\beta_3$)	14.103	0.0442	14.952	0.0448	15.825	0.0453	16.726	0.0459	17.653	0.0465
KM_3 ($K\beta_1$)	14.111	0.0865	14.961	0.0876	15.835	0.0886	16.738	0.0898	17.667	0.0909
KM_4 ($K\beta_5^{II}$)		0.0		0.0		0.0		0.0	17.815	0.0002
KM_5 ($K\beta_5^{I}$)		0.0		0.0		0.0		0.0	17.818	0.0003
K_{MM}	13.819	0.0010	14.639	0.0010	15.478	0.0011	16.345	0.0012	17.237	0.0013
KN_2 ($K\beta_2^{II}$)	14.311	0.0044	15.185	0.0052	16.084	0.0058	17.013	0.0063	17.968	0.0067
KN_3 ($K\beta_2^{I}$)	14.312	0.0085	15.186	0.0100	16.085	0.0114	17.016	0.0122	17.972	0.0130

Line	**Nb 92.91**		**Mo 95.94**		**Tc 97.00**		**Ru 101.07**		**Rh 102.90**	
KL_2 ($K\alpha_2$)	16.521	0.2880	17.374	0.2874	18.251	0.2868	19.150	0.2863	20.074	0.2861
KL_3 ($K\alpha_1$)	16.615	0.5499	17.479	0.5480	18.367	0.5463	19.279	0.5444	20.216	0.5428
K_{LM}	16.147	0.0008	16.975	0.0008	17.823	0.0008	18.694	0.0007	19.589	0.0007
KM_2 ($K\beta_3$)	18.607	0.0471	19.590	0.0476	20.599	0.0481	21.634	0.0485	22.699	0.0490
KM_3 ($K\beta_1$)	18.623	0.0919	19.607	0.0929	20.619	0.0937	21.657	0.0947	22.724	0.0953
KM_4 ($K\beta_5^{II}$)	18.778	0.0002	19.769	0.0002	20.788	0.0002	21.834	0.0003	22.908	0.0003
KM_5 ($K\beta_5^{I}$)	18.781	0.0003	19.773	0.0003	20.791	0.0003	21.838	0.0004	22.913	0.0004
K_{MM}	18.154	0.0015	19.103	0.0016	20.075	0.0018	21.072	0.0019	22.097	0.0018
KN_2 ($K\beta_2^{II}$)	18.950	0.0069	19.961	0.0072	21.001	0.0075	22.070	0.0078	23.168	0.0080
KN_3 ($K\beta_2^{I}$)	18.956	0.0135	19.967	0.0140	21.007	0.0146	22.076	0.0151	23.174	0.0156